

This is an Open Access document downloaded from ORCA, Cardiff University's institutional repository:<https://orca.cardiff.ac.uk/id/eprint/143677/>

This is the author's version of a work that was submitted to / accepted for publication.

Citation for final published version:

Carandini, Tiziana, Mancini, Matteo, Bogdan, Iulia, Rae, Charlotte L, Barritt, Andrew W, Clerico, Marinella, Sethi, Arjun, Harrison, Neil, Rashid, Waqar, Scarpini, Elio, Galimberti, Daniela, Bozzali, Marco and Cercignani, Mara 2021. In vivo evidence of functional disconnection between brainstem monoaminergic nuclei and brain networks in multiple sclerosis. *Multiple Sclerosis and Related Disorders* 56, 103224. 10.1016/j.msard.2021.103224

Publishers page: <https://doi.org/10.1016/j.msard.2021.103224>

Please note:

Changes made as a result of publishing processes such as copy-editing, formatting and page numbers may not be reflected in this version. For the definitive version of this publication, please refer to the published source. You are advised to consult the publisher's version if you wish to cite this paper.

This version is being made available in accordance with publisher policies. See <http://orca.cf.ac.uk/policies.html> for usage policies. Copyright and moral rights for publications made available in ORCA are retained by the copyright holders.



In vivo evidence of functional disconnection between brainstem monoaminergic nuclei and brain networks in multiple sclerosis

Tiziana Carandini^{1,2,3,*}, Matteo Mancini^{1,4,5}, Iulia Bogdan¹, Charlotte L Rae⁶, Andrew W Barritt¹, Marinella Clerico⁷, Arjun Sethi⁸, Neil Harrison⁹, Waqar Rashid¹, Elio Scarpini^{2,3}, Daniela Galimberti^{2,3}, Marco Bozzali^{1,10}, and Mara Cercignani^{1,11}.

¹Department of Neuroscience, Brighton and Sussex Medical School, University of Sussex, UK.

²Fondazione IRCCS Ca' Granda Ospedale Maggiore Policlinico, Milan, Italy

³University of Milan, Dino Ferrari Center, Milan, Italy.

⁴NeuroPoly Lab, Polytechnique Montreal, Montreal, Canada.

⁵CUBRIC, Cardiff University, Cardiff, UK.

⁶School of Psychology, University of Sussex, UK.

⁷Clinical and Biological Sciences Department, University of Torino, Orbassano (TO) 10043, Italy

⁸Psychiatry, Psychology & Neuroscience, King's College London, UK.

⁹Department of Psychology and Department of Medicine, Cardiff, UK.

¹⁰'Rita Levi Montalcini' Department of Neuroscience, University of Torino, Turin, Italy

¹¹Neuroimaging Laboratory, Santa Lucia Foundation IRCCS, Rome, Italy.

***Corresponding Author:**

Tiziana Carandini

Fondazione IRCCS Ca' Granda Ospedale Maggiore Policlinico, Milan, Italy

Email: tizianacarandini@gmail.com

Telephone: +39 02 5503 3845

ORCID: 0000-0002-0568-7580

Abstract word count: 291

Text word count: 3170

Abstract

Background: brainstem monoaminergic (dopaminergic, noradrenergic, and serotonergic) nuclei (BrMn) contain a variety of ascending neurons that diffusely project to the whole brain, crucially regulating normal brain function. BrMn are directly affected in multiple sclerosis (MS) by inflammation and neurodegeneration. Moreover, inflammation reduces the synthesis of monoamines. Aberrant monoaminergic neurotransmission contributes to the pathogenesis of MS and explains some clinical features of MS. We used resting-state functional MRI (RS-fMRI) to characterize abnormal patterns of BrMn functional connectivity (FC) in MS.

Methods: BrMn FC was studied with multi-echo RS-fMRI in n=68 relapsing-remitting MS patients and n=39 healthy controls (HC), by performing a seed-based analysis, after producing standard space seed masks of the BrMn. FC was assessed between ventral tegmental area (VTA), locus coeruleus (LC), median raphe (MR), dorsal raphe (DR), and the rest of the brain and compared between MS patients and HC. Between-group comparisons were carried out only within the main effect observed in HC, setting $p < 0.05$ family-wise-error corrected (FWE).

Results: in HC VTA displayed functionally connectivity with the core regions of the default-mode network. As compared to HC, MS patients showed altered FC between VTA and posterior cingulate cortex ($p < 0.05_{FWE}$). LC displayed FC with core regions of the executive-control network with a reduced functional connection between LC and right prefrontal cortex in MS patients ($p < 0.05_{FWE}$). Raphe nuclei was functionally connected with cerebellar cortex, with a significantly lower FC between these nuclei and cerebellum in MS patients, as compared to HC ($p < 0.05_{FWE}$).

Conclusions: our study demonstrated in MS patients a functional disconnection between BrMn and cortical/subcortical efferent targets of central brain networks, possibly due to a loss or a dysregulation of BrMn neurons. This adds new information about how monoaminergic systems contribute to MS pathogenesis and suggests new potential therapeutic targets.

Keywords

Multiple sclerosis, monoamines, monoaminergic systems, resting-state fMRI, functional connectivity

Abbreviations

BA = Brodmann area; BrMn = brainstem monoaminergic nuclei; CNS = central nervous system; DMN = default mode network; DR = dorsal raphe; ECN = executive control network; EDSS = expanded disease status score; EPI = echo-planar imaging; ESS = Epworth Sleepiness Scale; FC = functional connectivity; GM = grey matter; HADS-D = Hospital Anxiety and Depression Scale; HC = healthy controls; ICA = independent component analysis; LC = locus coeruleus; ME-ICA = multi-echo independent component analysis; MNI = Montreal Neurological Institute; MR = median raphe; MS = multiple sclerosis; PCC = posterior cingulate cortex; PFC = prefrontal cortex; RR-MS = relapsing-remitting MS; RS-fMRI = resting-state functional magnetic resonance imaging; SDMT = symbol digit modalities test; SPM = Statistical Parametric Mapping; TE = echo-time; TIV = total intracranial volume; VBM = voxel-based morphometry; VTA = ventral tegmental area; WM = white matter; WM-LL = WM lesion-load

1. Introduction

Brainstem monoaminergic nuclei (BrMn) encompass the dopaminergic ventral tegmental area (VTA), the noradrenergic locus coeruleus (LC), and the serotonergic median (MR) and dorsal (DR) raphe. BrMn project diffusely to the whole central nervous system (CNS), crucially regulating normal brain function, particularly arousal, mood, reward, and cognition (Bianciardi et al., 2016). Moreover, monoamines interact with cell-receptors of both nervous and immune systems and modulate neuroimmune interactions within the central nervous system and the periphery (Carandini et al., 2021a). Monoaminergic pathways are dysregulated in various neurological and psychiatric disorders, and are the targets for several clinically-useful drugs (Bär et al., 2016).

In multiple sclerosis (MS), monoamines pathways are dysfunctional as a result of both, the direct effect of inflammation, and the indirect effect of structural brain damage (Carandini et al., 2021a; Levite et al., 2017; Malinova et al., 2018; Manjaly et al., 2019; Melnikov et al., 2018). Inflammation-induced reduction of monoamine synthesis promotes a pro-inflammatory status in immune cells, and suppresses anti-inflammatory pathways (Melnikov et al., 2018). The brainstem is also a target for MS pathology (Reich et al., 2018) and lesions in monoaminergic pathways may occur as a result of BrMn damage or disconnection mechanism (Gadea, 2004; Polak et al., 2011; Tortorella et al., 2006). By using diffusion-tractography, we have recently demonstrated axonal damage within selective monoaminergic fibre-tracts projecting from BrMn in MS patients, in comparison to healthy controls (HC) (Carandini et al., 2021b). We speculated that axonal loss within monoaminergic fibre-tracts may alter/reduce monoaminergic transmission, possibly dysregulating monoaminergic pathways and leading to functional reorganization of cortical brain networks (Carandini et al., 2021b; Dobryakova et al., 2015).

An indirect measure of the dysfunction of monoaminergic pathways in MS can be obtained by using resting-state functional-magnetic resonance imaging (RS-fMRI), which detects the correlation between spontaneous fluctuations in neuronal activity at distant locations. RS-fMRI has been used to measure functional connectivity (FC) between BrMn and other brain areas (Bär et al., 2016; Bianciardi et al., 2016; Hahn et al., 2012; Serra et al., 2018). Since neuronal loss within a specific nucleus alters FC with its projection areas, RS-fMRI provides an indirect measure of neurodegeneration (Serra et al., 2018). In MS brains, impaired FC may also be due to dissemination of white matter (WM) lesions throughout the brain leading to WM-tract disconnection and reorganization of monoaminergic brain networks (Soares et al., 2020).

In this study, we used RS-fMRI in order to characterize abnormal patterns of FC between BrMn and the rest of the brain in a cohort of patients with MS, as compared to HC. Given the small size of BrMn and to minimise artefacts, a multi-echo acquisition was used(Kundu et al., 2017; Poser et al., 2006) and a seed-based-analysis was performed, as recently described(Bär et al., 2016; Serra et al., 2018).

2. Material and Methods

2.1 Participants

Sixty-eight patients with relapsing-remitting MS (RR-MS)(Thompson et al., 2018) and thirty-nine age- and sex-matched HC were recruited from the Brighton and Sussex Universities Hospitals Trust MS-clinic, United Kingdom. MS patients were the same that were used in two previously published studies by our group(Carandini et al., 2021b; Cercignani et al., 2021). Particularly, we included patients between 18 and 55 years-old with an expanded disease status score (EDSS) <6.5(Kurtzke, 1983), and without a history of other neurological diseases, psychiatric conditions and/or clinically significant disorders. Since mood and sleep disturbances may alter brainstem function, the Hospital Anxiety and Depression Scale (HADS-D) and the Epworth Sleepiness Scale (ESS) were used to exclude participants with evidence of depression and those likely to suffer from sleep disorders at the suggested cut-off of 11 and 10, respectively(Popp et al., 2017; Watson et al., 2014). MS patients were also screened for cognitive impairment, using the symbol digit modalities test (SDMT) of the brief international cognitive assessment for MS, which evaluates the speed of information processing(Langdon et al., 2012). Patients who had received steroid treatment or experienced a clinical relapse within the previous 4 weeks were excluded, as well as those in which MS-treatment had been changed within that same interval. HC were aged between 18 and 70 and did not have any significant medical disorders. All participants who had been on treatment with hypnotics within the last 4 weeks prior to their enrolment, on recreational drugs, or with a known alcohol abuse were excluded.

Ethical approvals were obtained from the London-Surrey Borders Research Ethics Committee (REC reference 17/LO/0081) and the local Brighton and Sussex Medical School-Research Governance and Ethics Committee (REC reference 14/014/HAR).

Written informed consent was obtained from all participants before study initiation according to the declaration of Helsinki.

2.2 MRI acquisition

MRI data were acquired on a 1.5T Siemens Magnetom Avanto scanner (Siemens Healthcare Solutions, Erlangen, Germany) equipped with a 32-channel head-coil, at the Clinical Imaging Sciences Centre of the University of Sussex, UK. The full examination included: 1) Dual-echo turbo-spin-echo (TSE): TE=11/86ms, TR=3040ms, echo-train-length=6, flip-angle=150°, FoV=220x192; matrix=256x224; slice-thickness=5mm; 2) Fast fluid-attenuated inversion recovery (FLAIR): TE=87ms, TR=8000ms, TI=2500ms, flip-angle=150°, echo-train-length=17, same resolution as the dual echo; 3) Volumetric high-resolution T1-weighted magnetization prepared rapid gradient-echo (MPRAGE): TE=3.57ms; TR=27.30ms; TI=100ms; flip-angle=70°; FoV=256x240mm²; matrix=254x40; slice-thickness=1mm); 4) T2*-weighted multi-echo echo-planar imaging (EPI) for RS-fMRI(Poser et al., 2006) (TE=15, 34, 54ms; TR=2570ms; flip-angle=90°; resolution=3.7x3.75x4.49mm; matrix-size=64x64; 31 axial slices; 185 volumes). The session also included diffusion-weighted MRI, as described in (Carandini et al., 2021b). During acquisition, subjects were instructed to keep their eyes closed, stay motionless, awake, without thinking of anything.

2.3 Pre-processing and acquisition of RS-fMRI data

To minimize motion artefacts and given the proximity of BrMn to large vessels and ventricles, a multi-echo independent component analysis (ME-ICA) was used for RS-fMRI data de-noising. ME-ICA(Kundu et al., 2017) utilizes the BOLD T2*-signal and combines a multi-echo RS-fMRI acquisition(Poser et al., 2006) with independent component analysis (ICA). Component-level echo-time (TE) dependence is measured with the two F-statistics κ and ρ , which respectively indicate BOLD and non-BOLD component weights by fitting the signal changes across TEs with two alternative models: one TE-dependent and one TE-independent. The resulting summary scores allow resting-state signals to be separated from non-BOLD-like components that are used as noise regressors for data cleaning(Kundu et al., 2014).

Multi-echo data pre-processing was conducted using the AFNI-2018 tool *meica.py*, version 3.2(Cox, 1996; Kundu et al., 2014, 2013). Pre-processing included volume re-alignment, time-series de-spiking and slice time correction. Functional data were optimally combined(Posse et al., 1999) and multi-echo principal components analysis was first applied to the optimally-combined dataset to reduce data dimensionality. Spatial-ICA was applied and the independent component time-series were fit to the pre-processed time-series to generate ICA weights for each echo. ICA-weight was fit to the linear TE-dependent and TE-independent models to generate the κ and ρ metrics that were finally used to identify non-BOLD-like components to be regressed out of the optimally-combined dataset, together with the average

WM and cerebrospinal fluid signals. Further details on ME-ICA can be found in: (Dipasquale et al., 2017; Kundu et al., 2015).

2.4 Seed-based analysis

Standard-space seed masks of VTA, DR, MR, and left/right LC were produced using the Harvard Ascending Arousal Network Atlas in Montreal Neurological Institute (MNI)_152_1 mm space (<https://www.martinos.org/>), as recently described (Edlow et al., 2012; Serra et al., 2018) (**Fig.1**). To minimize the partial volume contamination from surrounding nuclei, the mean time course within each seed region was extracted from unsmoothed data for every participant (averaged for left and right sides). Smoothed data were regressed voxel-wise against these time courses in a first-level Statistical Parametric Mapping 12 (SPM12; Wellcome Department of Imaging Neuroscience; www.fil.ion.ucl.ac.uk/spm) analysis (Olivito et al., 2017; Serra et al., 2018).

2.6 Statistical analyses

Statistical analyses were performed using SPSS Statistics v25.0 (SPSS Inc., Chicago, Ill., USA). Between-group comparisons of demographic variables were performed using Mann-Whitney U tests or chi-square tests, as appropriate. Comparisons of FC between MS patients without and with antidepressant medications were tested using Mann-Whitney U tests. Statistical threshold was set to $p < 0.05$.

The following separate RS-fMRI second-level SPM12 analyses were performed for each brainstem-nucleus: (1) average within-group FC (main effect) in HC (one-sample t-test); (2) comparison of FC between HC and MS patients (two-sample t-test). Results of FC in HC are reported for $p < 0.001_{\text{uncorrected}}$, while comparisons and correlations were carried out only within the main effect found in HC (small-volume correction), setting the family wise-error p ($p_{\text{FWE}} < 0.05$, corrected at peak level). In all RS-fMRI analyses, age, gender, and total intracranial volume (TIV) were entered as covariates of no interest.

3. Results

3.1 Participants' characteristics

The main characteristics of the included population are summarized in **Table 1**. Age and gender distribution did not differ significantly between MS patients and HC. Among patients, 76.5% were under MS specific treatment, and 19.1% were undertaking low doses of

antidepressants. Patients did not suffer from depression, anxiety or daytime-sleepiness. SDMT score was below 38 only in 8 patients.

3.2 RS-fMRI analysis

3.2.1 BrMn FC in HC

RS-fMRI data in HC (main effects) are summarized in **Figure 2** and **Table 2**. VTA was functionally connected to the posterior cingulate cortex (PCC) [right Brodmann area (BA) 23; left BA31], inferior parietal lobule [bilateral BA39], parahippocampal cortex [left BA36], hippocampus [left BA54], thalamus [left BA50], prefrontal cortex (PFC) [left BA10], brainstem, and cerebellum [vermis]. LC showed FC with the PFC [right BA10], insula [right BA13], thalamus [right BA50], brainstem, and left cerebellar lobule VII. MR displayed FC with the PCC [right BA31], inferior and superior parietal lobules [bilateral BA39; bilateral BA7], amygdala [left BA53], brainstem, and multiple cerebellar regions. Conversely, DR was connected with the brainstem, only.

3.2.2 Comparisons of BrMn FC in MS patients and HC

Comparisons of BrMn FC in MS patients and HC are summarized in **Figure 3** and **Table 3**. Compared to HC, MS patients showed lower FC between VTA and bilateral PCC [right BA23 and left BA31], and between LC and PFC [right BA10] and brainstem. Reduced FC between both raphe nuclei and the cerebellum was found in patients, as compared to HC, particularly between MR and left Crus I and right lobules V-VI, and between DR and right Crus II. The opposite contrast (MS patients>HC) did not return any significant results for every BrMn considered.

3.4 Antidepressant medications

MS patients who were taking low doses of antidepressant medications did not show differences in BrMn FC, compared to those who were not ($p>0.05$ for all comparisons).

4. Discussion

The interactions of BrMn-located monoaminergic neurons with cortical and subcortical regions are crucial to coordinate cognitive and behavioral functions in the human brain. Brainstem damage and atrophy occur early during MS course, possibly as a result of local inflammation, retrograde degeneration through WM lesions, mitochondrial dysfunction, and iron accumulation (Berg et al., 2000; Tortorella et al., 2006). Alterations in monoaminergic

systems have been described in MS patients and have been linked to various symptoms of MS, such as fatigue, depression, and cognitive impairment (Carandini et al., 2021a; Cercignani et al., 2021; Dobryakova et al., 2015; Manjaly et al., 2019). The present study reveals functional disconnection between BrMn and central brain networks in patients with RR-MS, in comparison to HC. We focused on VTA, LC, and raphe nuclei (DR and MR) as the main brainstem source of dopaminergic, noradrenergic, and serotonergic neurons, respectively. Among dopaminergic pathways, we did not consider the nigrostriatal system – encompassing dopaminergic cells from the *substantia nigra pars compacta* – which is part of the basal ganglia loop, but only the mesocorticolimbic system, originating from VTA.

In line with previous studies (Bär et al., 2016; Serra et al., 2018), the analysis of BrMn FC in HC revealed specific dopaminergic and serotonergic functional connections with core regions of the default mode network (DMN). The DMN encompasses the precuneus/PCC, anterior cingulate cortex and temporo-parietal junction areas, and constitutes the most relevant non-motor central network in the human brain. DMN expresses dopaminergic/serotonergic receptors and these monoamines modulate DMN connectivity (Conio et al., 2019; Hahn et al., 2012; Nagano-Saito et al., 2017). Particularly, Carbonell et al. found that dopaminergic precursor depletion impairs DMN efficiency (Carbonell et al., 2014). Cole et al. reported that levodopa and haloperidol challenges, respectively, increase or decrease the FC between the midbrain and the DMN (Cole et al., 2013). Nagano-Saito et al. reported that the posterior distribution of D2/D3 dopaminergic receptors coincides primarily with the posterior portion of the DMN (Nagano-Saito et al., 2017). Moreover, a PET-fMRI study demonstrated a relationship between serotonergic-receptor binding levels and BOLD signal in the DMN (Hahn et al., 2012). Our findings in HC confirmed that VTA and MR are connected to the DMN, and possibly modulate its activity. Conversely, in line with (Bianciardi et al., 2016), DR did not show significant functional connections with it. Moreover, we confirmed the limited influence of the LC on DMN activity (Bär et al., 2016; Kline et al., 2016), which was instead functionally connected with the right PFC and insula – part of the executive control network (ECN) – and thalamus. The ECN encompasses bilateral PFC, inferior parietal lobes, anterior-cingulate/supplementary motor area, and bilateral insular cortices, and is involved in cognitive flexibility, working memory and attention. LC is known to modulate the ECN activity, and disconnections in this functional network have been described (Bär et al., 2016; Heine et al., 2012; Liu et al., 2017). All BrMn revealed FC with the cerebellar cortex, as previously observed (Bär et al., 2016). The functional topography of the cerebellum can be divided into zones depending on the connectivity with sensorimotor vs. multimodal association cortices: the

lobule V-VI is connected with sensorimotor zones, whereas the lobule VII (encompassing Crus I-Crus II-lobule VIIb) with the PFC and posterior-parietal cortex(O'Reilly et al., 2010). Interestingly, the LC was functionally connected with the left-lobule VII (controlateral to the right PFC), while MR/DR showed FC with both lobules V-VI/VII. These findings confirm the active role of MC systems in modulating cerebellar activity.

Our study provided a comprehensive characterization of BrMn patterns of FC in patients with MS. We observed functional disconnection in MS patients between VTA – but not raphe nuclei – and the DMN region with the highest expression of dopaminergic receptors: the PCC(Nagano-Saito et al., 2017). In MS, alterations in the DMN connectivity are highly involved in cognitive performance, fatigue, and depression(Rocca et al., 2010). Our findings suggest that the disconnection reported in MS within the DMN might be at least partially due to VTA dysfunction. Conversely, serotonergic modulation of the DMN did not result different in MS patients, as compared to HC. Moreover, LC disconnection with the right PFC in MS patients possibly reflects an altered noradrenergic modulation of the ECN. The laterality in our results may be explained by the well-known ECN lateralization, with the left part more implicated in cognitive functions, and the right more related to somesthetic/nociceptive processing(Heine et al., 2012). MS patients revealed also a functional disconnection between raphe nuclei – particularly the MR – and cerebellar cortex (both lobules V-VI and VII). Serotonergic-fibres richly modulate cerebellar functioning(Oostland and van Hoof, 2016), suggesting that the known alterations in cerebellar connectivity in MS may be partially explained by dysfunctions in the serotonergic projections from raphe nuclei. Our results confirmed and enriched the findings by Carotenuto et al. on a larger cohort of MS patients; these authors recently reported increased FC between the dorsal raphe and the PFC, decreased FC between the VTA and the PFC, and decreased betweenness centrality (a measure of the importance of a given node within a network) for the brainstem in MS patients, as compared to HC(Carotenuto et al., 2020). Similarly, by using proton-MR-spectroscopy, Gadea et al. reported a reduction of N-acetyl-aspartate/creatine ratio in the pontine normal-appearing WM of a group of early RR-MS patients, possibly representing an indirect measure of structural damage of LC cells or its projections(Gadea, 2004).

We hypothesized that the functional disconnections observed in MS patients between BrMn and central brain network could result from three main processes, possibly occurring simultaneously: 1) axonal loss secondary to WM lesions either within WM tracts projecting from BrMn or disseminated throughout the brain; 2) regional grey matter (GM) atrophy leading to neurodegeneration of central brain networks' cortical neurons; 3) direct

inflammatory/neurodegenerative early damage of BrMn. By using diffusion-tractography, we recently demonstrated on the same cohort of MS patients that was used in the present study a selective WM damage along specific fibre tracts projecting from BrMn, particularly within the dopaminergic-mesolimbic pathway, noradrenergic-projections to PFC and serotonergic-projections to cerebellum(Carandini et al., 2021b). We believe that axonal loss along monoaminergic pathways may primarily drive the monoaminergic functional disconnection and reorganization of central brain networks(Soares et al., 2020). In the same study(Carandini et al., 2021b), we also demonstrated that regional GM volumes in MS patients are significantly reduced only in bilateral thalamus(Filippi and Rocca, 2011), thus making unlikely a contribution of GM atrophy in determining monoaminergic functional disconnection. Similarly, only 1 out of 68 MS patients showed visible macroscopic lesions in the brainstem. This suggests that local WM damage did not significantly contribute to our results, though the detection of macroscopic brainstem lesions may be limited by the relatively low resolution of our MRI images (about 5mm of thickness)(Carandini et al., 2021b). Further studies are needed to better characterize the structural damage occurring to BrMn in MS.

This study suffers from some limitations. First of all, BrMn are very small, difficult to identify on MRI, and located in proximity to large vessels and ventricles. Thus, some of our results might be affected by partial volume effect with neighboring structures of the brainstem and by respiration and pulsatility artifacts. We tried to minimize these potential biases, by conducting a ME-ICA for RS-fMRI data de-noising, an approach found to be much more robust than alternative ones, particularly in clinical populations(Dipasquale et al., 2017). Moreover, we are aware that the definition of BrMn using an atlas in standard space (due to the difficulties in identifying each nucleus on individual scans) is less accurate than registering the standard ROI to each participant's scan. Macroscopic atrophy of the BrMn might also have influenced our results(Serra et al., 2018). Nonetheless, it is not possible to measure the volume of each nucleus independently, and thus adjust for this potential confound. Notably, 15 out of 68 MS patients were on low doses of antidepressants (i.e. Selective Serotonin–Norepinephrine Reuptake Inhibitors or Tricyclic), which are known to alter the levels of monoamines within the CNS. However, no differences in BrMn FC were found between MS patients who were on antidepressants and those who were not. Finally, the present study has a cross-sectional design. Longitudinal studies are needed to analyse the relationship between BrMn FC changes in MS patients.

In conclusion, we confirmed the functional integration of BrMn within central brain networks that are crucial for normal brain functioning and provided evidence in MS patients of a functional disconnection between these nuclei and central brain networks that are involved in MS pathology, possibly due to a loss or a dysregulation of BrMn neurons. These data support the hypothesis of a major contribution of monoamines in MS pathogenesis and suggest a direct clinical implication of monoaminergic dysfunction for some clinical features of MS, particularly fatigue, depression, and cognitive impairment. The evidence of functional disconnection between BrMn and central brain networks in MS also provides a rationale for proposing therapeutic strategies to activate, replace or supplement monoaminergic transmission within the CNS of MS patients.

CRedit authorship contribution statement: **Tiziana Carandini:** Conceptualization, Formal analysis, Writing - original draft. **Matteo Mancini:** Conceptualization, Formal analysis, Writing - original draft. **Iulia Bogdan:** Project administration, Funding acquisition, Formal analysis. **Charlotte L Rae:** Formal analysis. **Andrew W Barritt:** Project administration, Formal analysis. **Marinella Clerico:** Writing - review & editing. **Arjun Sethi:** Formal analysis. **Neil Harrison:** Writing - review & editing. **Waqar Rashid:** Project administration, Formal analysis. **Elio Scarpini:** Writing - review & editing. **Daniela Galimberti:** Writing - review & editing. **Marco Bozzali:** Conceptualization, Writing - review & editing. **Mara Cercignani:** Conceptualization, Formal analysis, Project administration, Funding acquisition, Writing - original draft.

Declaration of Competing Interests: the author(s) declared the following potential conflicts of interest with respect to the research, authorship, and/or publication of this article: MM was funded by the Wellcome Trust through a Sir Henry Wellcome Postdoctoral Fellowship (213722/Z/18/Z). IB received travel and study support from Biogen, Merck, Novartis and Sanofi-Genzyme. NH has served on scientific advisory boards for Janssen and GSK Pharmaceuticals, is in receipt of grant funding from the Wellcome Trust and has received research funding support from Janssen Pharmaceuticals and Action for ME. MB received honoraria from Biogen and Merck, and research support from the Italian Ministry of Health. MC received royalties from Taylor and Francis from the publication of a book, research funding from Wellcome Trust, Motor Neuron Disease Association, and the Academy of Medical Sciences. She also received institutional support from the University of Sussex and the

University of Brighton. TC, CLR, AWM, MC, AS, WR, ES, and DG report no potential conflicts of interest.

Funding: the authors have not declared a specific grant for this research from any funding agency in the public, commercial or not-for-profit sectors.

References

- Bär, K.-J., de la Cruz, F., Schumann, A., Koehler, S., Sauer, H., Critchley, H., Wagner, G., 2016. Functional connectivity and network analysis of midbrain and brainstem nuclei. *NeuroImage* 134, 53–63. <https://doi.org/10.1016/j.neuroimage.2016.03.071>
- Berg, D., Supprian, T., Thomae, J., Warmuth-Metz, M., Horowski, A., Zeiler, B., Magnus, T., Rieckman, P., Becker, G., 2000. Lesion pattern in patients with multiple sclerosis and depression. *Multiple Sclerosis* 6, 156–162. <https://doi.org/10.1191/135245800701566016>
- Bianciardi, M., Toschi, N., Eichner, C., Polimeni, J.R., Setsompop, K., Brown, E.N., Hämäläinen, M.S., Rosen, B.R., Wald, L.L., 2016. In vivo functional connectome of human brainstem nuclei of the ascending arousal, autonomic, and motor systems by high spatial resolution 7-Tesla fMRI. *Magn Reson Mater Phy* 29, 451–462. <https://doi.org/10.1007/s10334-016-0546-3>
- Carandini, T., Cercignani, M., Galimberti, D., Scarpini, E., Bozzali, M., 2021a. The distinct roles of monoamines in multiple sclerosis: A bridge between the immune and nervous systems? *Brain, Behavior, and Immunity* S0889159121000957. <https://doi.org/10.1016/j.bbi.2021.02.030>
- Carandini, T., Mancini, M., Bogdan, I., Rae, C.L., Barritt, A.W., Sethi, A., Harrison, N., Rashid, W., Scarpini, E., Galimberti, D., Bozzali, M., Cercignani, M., 2021b. Disruption of brainstem monoaminergic fibre tracts in multiple sclerosis as a putative mechanism for cognitive fatigue: a fixel-based analysis. *NeuroImage: Clinical* 30, 102587. <https://doi.org/10.1016/j.nicl.2021.102587>
- Carbonell, F., Nagano-Saito, A., Leyton, M., Cisek, P., Benkelfat, C., He, Y., Dagher, A., 2014. Dopamine precursor depletion impairs structure and efficiency of resting state brain functional networks. *Neuropharmacology* 84, 90–100. <https://doi.org/10.1016/j.neuropharm.2013.12.021>
- Carotenuto, A., Wilson, H., Giordano, B., Caminiti, S.P., Chappell, Z., Williams, S.C.R., Hammers, A., Silber, E., Brex, P., Politis, M., 2020. Impaired connectivity within

- neuromodulatory networks in multiple sclerosis and clinical implications. *J Neurol*.
<https://doi.org/10.1007/s00415-020-09806-3>
- Cercignani, M., Dipasquale, O., Bogdan, I., Carandini, T., Scott, J., Rashid, W., Sabri, O., Hesse, S., Rullmann, M., Lopiano, L., Veronese, M., Martins, D., Bozzali, M., 2021. Cognitive fatigue in multiple sclerosis is associated with alterations in the functional connectivity of monoamine circuits. *Brain Communications* 3, fcab023. <https://doi.org/10.1093/braincomms/fcab023>
- Cole, D.M., Oei, N.Y.L., Soeter, R.P., Both, S., van Gerven, J.M.A., Rombouts, S.A.R.B., Beckmann, C.F., 2013. Dopamine-Dependent Architecture of Cortico-Subcortical Network Connectivity. *Cerebral Cortex* 23, 1509–1516. <https://doi.org/10.1093/cercor/bhs136>
- Conio, B., Martino, M., Magioncalda, P., Escelsior, A., Inglese, M., Amore, M., Northoff, G., 2019. Opposite effects of dopamine and serotonin on resting-state networks: review and implications for psychiatric disorders. *Mol Psychiatry*. <https://doi.org/10.1038/s41380-019-0406-4>
- Cox, R.W., 1996. AFNI: Software for Analysis and Visualization of Functional Magnetic Resonance Neuroimages. *Computers and Biomedical Research* 29, 162–173. <https://doi.org/10.1006/cbmr.1996.0014>
- Dipasquale, O., Sethi, A., Laganà, M.M., Baglio, F., Baselli, G., Kundu, P., Harrison, N.A., Cercignani, M., 2017. Comparing resting state fMRI de-noising approaches using multi- and single-echo acquisitions. *PLoS ONE* 12, e0173289. <https://doi.org/10.1371/journal.pone.0173289>
- Dobryakova, E., Genova, H.M., DeLuca, J., Wylie, G.R., 2015. The Dopamine Imbalance Hypothesis of Fatigue in Multiple Sclerosis and Other Neurological Disorders. *Front. Neurol.* 6. <https://doi.org/10.3389/fneur.2015.00052>
- Edlow, B.L., Takahashi, E., Wu, O., Benner, T., Dai, G., Bu, L., Grant, P.E., Greer, D.M., Greenberg, S.M., Kinney, H.C., Folkerth, R.D., 2012. Neuroanatomic Connectivity of the Human Ascending Arousal System Critical to Consciousness and Its Disorders. *J Neuropathol Exp Neurol* 71, 531–546. <https://doi.org/10.1097/NEN.0b013e3182588293>
- Filippi, M., Rocca, M.A., 2011. The role of magnetic resonance imaging in the study of multiple sclerosis: diagnosis, prognosis and understanding disease pathophysiology. *Acta Neurol Belg* 111, 89–98.
- Gadea, M., 2004. Spectroscopic axonal damage of the right locus coeruleus relates to selective attention impairment in early stage relapsing-remitting multiple sclerosis. *Brain* 127, 89–98. <https://doi.org/10.1093/brain/awh002>

- Hahn, A., Wadsak, W., Windischberger, C., Baldinger, P., Hoflich, A.S., Losak, J., Nics, L., Philippe, C., Kranz, G.S., Kraus, C., Mitterhauser, M., Karanikas, G., Kasper, S., Lanzenberger, R., 2012. Differential modulation of the default mode network via serotonin-1A receptors. *Proceedings of the National Academy of Sciences* 109, 2619–2624. <https://doi.org/10.1073/pnas.1117104109>
- Heine, L., Soddu, A., Gómez, F., Vanhauzenhuysse, A., Tshibanda, L., Thonnard, M., Charland-Verville, V., Kirsch, M., Laureys, S., Demertzi, A., 2012. Resting State Networks and Consciousness. *Front. Psychology* 3. <https://doi.org/10.3389/fpsyg.2012.00295>
- Kline, R.L., Zhang, S., Farr, O.M., Hu, S., Zaborszky, L., Samanez-Larkin, G.R., Li, C.-S.R., 2016. The Effects of Methylphenidate on Resting-State Functional Connectivity of the Basal Nucleus of Meynert, Locus Coeruleus, and Ventral Tegmental Area in Healthy Adults. *Front. Hum. Neurosci.* 10. <https://doi.org/10.3389/fnhum.2016.00149>
- Kundu, P., Benson, B.E., Baldwin, K.L., Rosen, D., Luh, W.-M., Bandettini, P.A., Pine, D.S., Ernst, M., 2015. Robust resting state fMRI processing for studies on typical brain development based on multi-echo EPI acquisition. *Brain Imaging and Behavior* 9, 56–73. <https://doi.org/10.1007/s11682-014-9346-4>
- Kundu, P., Brenowitz, N.D., Voon, V., Worbe, Y., Vertes, P.E., Inati, S.J., Saad, Z.S., Bandettini, P.A., Bullmore, E.T., 2013. Integrated strategy for improving functional connectivity mapping using multiecho fMRI. *Proceedings of the National Academy of Sciences* 110, 16187–16192. <https://doi.org/10.1073/pnas.1301725110>
- Kundu, P., Santin, M.D., Bandettini, P.A., Bullmore, E.T., Petiet, A., 2014. Differentiating BOLD and non-BOLD signals in fMRI time series from anesthetized rats using multi-echo EPI at 11.7T. *NeuroImage* 102, 861–874. <https://doi.org/10.1016/j.neuroimage.2014.07.025>
- Kundu, P., Voon, V., Balchandani, P., Lombardo, M.V., Poser, B.A., Bandettini, P.A., 2017. Multi-echo fMRI: A review of applications in fMRI denoising and analysis of BOLD signals. *NeuroImage* 154, 59–80. <https://doi.org/10.1016/j.neuroimage.2017.03.033>
- Kurtzke, J.F., 1983. Rating neurologic impairment in multiple sclerosis: an expanded disability status scale (EDSS). *Neurology* 33, 1444–1452. <https://doi.org/10.1212/wnl.33.11.1444>
- Langdon, D., Amato, M., Boringa, J., Brochet, B., Foley, F., Fredrikson, S., Hämäläinen, P., Hartung, H.-P., Krupp, L., Penner, I., Reder, A., Benedict, R., 2012. Recommendations for a Brief International Cognitive Assessment for Multiple Sclerosis (BICAMS). *Mult Scler* 18, 891–898. <https://doi.org/10.1177/1352458511431076>
- Levite, M., Marino, F., Cosentino, M., 2017. Dopamine, T cells and multiple sclerosis (MS). *J Neural Transm* 124, 525–542. <https://doi.org/10.1007/s00702-016-1640-4>

- Liu, K.Y., Marijatta, F., Hämmerer, D., Acosta-Cabronero, J., Düzel, E., Howard, R.J., 2017. Magnetic resonance imaging of the human locus coeruleus: A systematic review. *Neuroscience & Biobehavioral Reviews* 83, 325–355. <https://doi.org/10.1016/j.neubiorev.2017.10.023>
- Malinova, T.S., Dijkstra, C.D., de Vries, H.E., 2018. Serotonin: A mediator of the gut–brain axis in multiple sclerosis. *Mult Scler* 24, 1144–1150. <https://doi.org/10.1177/1352458517739975>
- Manjaly, Z.-M., Harrison, N.A., Critchley, H.D., Do, C.T., Stefanics, G., Wenderoth, N., Lutterotti, A., Müller, A., Stephan, K.E., 2019. Pathophysiological and cognitive mechanisms of fatigue in multiple sclerosis. *J Neurol Neurosurg Psychiatry* 90, 642–651. <https://doi.org/10.1136/jnnp-2018-320050>
- Melnikov, M., Rogovskii, V., Boyko, A., Pashenkov, M., 2018. The influence of biogenic amines on Th17-mediated immune response in multiple sclerosis. *Multiple Sclerosis and Related Disorders* 21, 19–23. <https://doi.org/10.1016/j.msard.2018.02.012>
- Nagano-Saito, A., Lissemore, J.I., Gravel, P., Leyton, M., Carbonell, F., Benkelfat, C., 2017. Posterior dopamine D2/3 receptors and brain network functional connectivity. *Synapse* 71, e21993. <https://doi.org/10.1002/syn.21993>
- Olivito, G., Clausi, S., Laghi, F., Tedesco, A.M., Baiocco, R., Mastropasqua, C., Molinari, M., Cercignani, M., Bozzali, M., Leggio, M., 2017. Resting-State Functional Connectivity Changes Between Dentate Nucleus and Cortical Social Brain Regions in Autism Spectrum Disorders. *Cerebellum* 16, 283–292. <https://doi.org/10.1007/s12311-016-0795-8>
- Oostland, M., van Hooft, J.A., 2016. Serotonin in the Cerebellum, in: Gruol, D.L., Koibuchi, N., Manto, M., Molinari, M., Schmahmann, J.D., Shen, Y. (Eds.), *Essentials of Cerebellum and Cerebellar Disorders*. Springer International Publishing, Cham, pp. 243–247. https://doi.org/10.1007/978-3-319-24551-5_31
- O'Reilly, J.X., Beckmann, C.F., Tomassini, V., Ramnani, N., Johansen-Berg, H., 2010. Distinct and Overlapping Functional Zones in the Cerebellum Defined by Resting State Functional Connectivity. *Cerebral Cortex* 20, 953–965. <https://doi.org/10.1093/cercor/bhp157>
- Polak, P.E., Kalinin, S., Feinstein, D.L., 2011. Locus coeruleus damage and noradrenaline reductions in multiple sclerosis and experimental autoimmune encephalomyelitis. *Brain* 134, 665–677. <https://doi.org/10.1093/brain/awq362>
- Popp, R.F.J., Fierlbeck, A.K., Knüttel, H., König, N., Rupprecht, R., Weissert, R., Wetter, T.C., 2017. Daytime sleepiness versus fatigue in patients with multiple sclerosis: A systematic review on the Epworth sleepiness scale as an assessment tool. *Sleep Medicine Reviews* 32,

95–108. <https://doi.org/10.1016/j.smrv.2016.03.004>

- Poser, B.A., Versluis, M.J., Hoogduin, J.M., Norris, D.G., 2006. BOLD contrast sensitivity enhancement and artifact reduction with multiecho EPI: parallel-acquired inhomogeneity-desensitized fMRI. *Magn Reson Med* 55, 1227–1235. <https://doi.org/10.1002/mrm.20900>
- Posse, S., Wiese, S., Gembris, D., Mathiak, K., Kessler, C., Grosse-Ruyken, M.L., Elghahwagi, B., Richards, T., Dager, S.R., Kiselev, V.G., 1999. Enhancement of BOLD-contrast sensitivity by single-shot multi-echo functional MR imaging. *Magn Reson Med* 42, 87–97. [https://doi.org/10.1002/\(sici\)1522-2594\(199907\)42:1<87::aid-mrm13>3.0.co;2-o](https://doi.org/10.1002/(sici)1522-2594(199907)42:1<87::aid-mrm13>3.0.co;2-o)
- Reich, D.S., Lucchinetti, C.F., Calabresi, P.A., 2018. Multiple Sclerosis. *N. Engl. J. Med.* 378, 169–180. <https://doi.org/10.1056/NEJMra1401483>
- Rocca, M.A., Valsasina, P., Absinta, M., Riccitelli, G., Rodegher, M.E., Misci, P., Rossi, P., Falini, A., Comi, G., Filippi, M., 2010. Default-mode network dysfunction and cognitive impairment in progressive MS. *Neurology* 74, 1252–1259. <https://doi.org/10.1212/WNL.0b013e3181d9ed91>
- Serra, L., D’Amelio, M., Di Domenico, C., Dipasquale, O., Marra, C., Mercuri, N.B., Caltagirone, C., Cercignani, M., Bozzali, M., 2018. In vivo mapping of brainstem nuclei functional connectivity disruption in Alzheimer’s disease. *Neurobiology of Aging* 72, 72–82. <https://doi.org/10.1016/j.neurobiolaging.2018.08.012>
- Soares, J.M., Conde, R., Magalhães, Ricardo, Marques, P., Magalhães, Rosana, Gomes, L., Gonçalves, Ó.F., Arantes, M., Sampaio, A., 2020. Alterations in functional connectivity are associated with white matter lesions and information processing efficiency in multiple sclerosis. *Brain Imaging and Behavior*. <https://doi.org/10.1007/s11682-020-00264-z>
- Thompson, A.J., Banwell, B.L., Barkhof, F., Carroll, W.M., Coetzee, T., Comi, G., Correale, J., Fazekas, F., Filippi, M., Freedman, M.S., Fujihara, K., Galetta, S.L., Hartung, H.P., Kappos, L., Lublin, F.D., Marrie, R.A., Miller, A.E., Miller, D.H., Montalban, X., Mowry, E.M., Sorensen, P.S., Tintoré, M., Traboulsee, A.L., Trojano, M., Uitdehaag, B.M.J., Vukusic, S., Waubant, E., Weinshenker, B.G., Reingold, S.C., Cohen, J.A., 2018. Diagnosis of multiple sclerosis: 2017 revisions of the McDonald criteria. *The Lancet Neurology* 17, 162–173. [https://doi.org/10.1016/S1474-4422\(17\)30470-2](https://doi.org/10.1016/S1474-4422(17)30470-2)
- Tortorella, P., Rocca, M.A., Colombo, B., Annovazzi, P., Comi, G., Filippi, M., 2006. Assessment of MRI abnormalities of the brainstem from patients with migraine and multiple sclerosis. *Journal of the Neurological Sciences* 244, 137–141. <https://doi.org/10.1016/j.jns.2006.01.015>
- Watson, T.M., Ford, E., Worthington, E., Lincoln, N.B., 2014. Validation of Mood Measures

for People with Multiple Sclerosis. *International Journal of MS Care* 16, 105–109.
<https://doi.org/10.7224/1537-2073.2013-013>

Table 1: Main demographic and clinical characteristics of the included population. Data are reported as mean \pm standard deviation, and number (percentage) for continuous and categorical variables, respectively.

	RR-MS	HC	<i>p</i>
n	68	39	
Age, years	43.3 \pm 7.7	40.1 \pm 15.5	0.07
Female	43 (63.2)	21 (53.8)	0.3
Disease duration, years	7.4 \pm 6.5		
EDSS, median (1st-3rd quartiles)	1.5 (1.0-3.0)		
MS-specific treatment			
<i>No treatment</i>	16 (23.5)		
<i>First line DMTs</i>	25 (36.8)		
<i>Second line DMTs</i>	27 (39.7)		
Antidepressants	15 (23.5)		
<i>SSRIs</i>	7 (10.3)		
<i>SNRIs</i>	3 (4.4)		
<i>TCAs</i>	5 (7.3)		
BICAMS-SDMT, median (1st-3rd quartiles)	49.0 (48.2-64.7)		
HADS-D, median (1st-3rd quartiles)	1.5 (1.0-4.0)		
ESS, median (1st-3rd quartiles)	4.0 (2.0-6.2)		

[Abbreviations = RR-MS: Relapsing-Remitting Multiple Sclerosis; HC: Healthy Controls; EDSS: Expanded Disability Status Scale; DMTs: Disease Modifying Therapies; SSRIs: Selective Serotonin Reuptake Inhibitors; SNRIs: Serotonin–Norepinephrine Reuptake Inhibitors; TCAs: Tricyclic Antidepressants; BICAMS-SDMT: Brief International Cognitive Assessment for MS-Symbol Digit Modalities Test; HADS-D: Hospital Anxiety Depression Scale; ESS: Epworth Sleepiness Scale.]

Table 2: Resting-state functional connectivity of brainstem monoaminergic nuclei in healthy controls (main effects). Results are reported for $p < 0.001$, uncorrected. Cluster extension (K_{extend}) indicates the number of contiguous voxels with voxel-wise statistic values.

Seed region	Connected region	MNI coordinates			BA	t-value	K_{extend}
		<i>x</i>	<i>y</i>	<i>z</i>			
VTA	PCC	6	-52	26	R 23	7.72	2920
	PCC	-6	-62	22	L 31	6.79	2920
	Inferior Parietal Lobule	-58	-60	22	L 39	3.92	517
	Inferior Parietal Lobule	50	-62	30	R 39	4.38	185
	Parahippocampal Cortex	-26	-4	-30	L 36	4.62	374
	Hippocampus	-24	-14	-24	L 54	4.17	374
	Thalamus	-10	-14	-2	L 50	4.59	134
	PFC	-4	52	-8	L 10	4.31	137
	Brainstem	2	-24	-20	-	67.35	934
	Cerebellum, Vermis	0	-64	-30	-	4.58	88
LC	PFC	32	54	6	R 10	5.13	162
	Insula	32	22	4	R 13	4.57	90
	Thalamus	6	-6	-2	R 50	4.20	170
	Brainstem	-6	-36	-28	-	37.35	2610
	Brainstem	6	-36	-28	-	36.90	2610
	Cerebellum, Left VII, Crus I	-42	-46	-40	-	5.28	164
MR	PCC	10	-62	38	R 31	3.99	147
	Inferior Parietal Lobule	-40	-52	42	L 39	5.03	117
	Inferior Parietal Lobule	38	-66	50	R 39	4.68	494
	Superior Parietal Lobule	-8	-74	42	L 7	4.47	160
	Superior Parietal Lobule	12	-66	46	R 7	4.05	147
	Amygdala	-20	-4	-22	L 53	3.59	183
	Brainstem	0	-32	-28	-	42.69	2831
	Cerebellum, Left VII, Crus I	-40	-56	-32	-	6.67	2831
	Cerebellum, Right VII, Crus I	34	-52	-36	-	5.70	1882
	Cerebellum Right V	18	-40	-20	-	5.32	1882
DR	Brainstem	0	-32	-18	-	69.36	2150

[Abbreviations: MNI: Montreal Neurological Institute; BA: Brodmann area; k_{extend} : cluster extension; L: left; R: right; VTA: ventral tegmental area; LC: locus coeruleus; MR: median raphe; DR: dorsal raphe; PCC: posterior cingulate cortex; PFC: prefrontal cortex]

Table 3: Brain regions showing a higher resting state-functional connectivity with brainstem monoaminergic nuclei in healthy controls as compared to relapsing-remitting multiple sclerosis patients. All comparisons were carried out within the main effect of healthy controls, setting $p < 0.05$ family-wise-error (FWE), corrected at peak level. Cluster extension (K_{extend}) indicates the number of contiguous voxels with voxel-wise statistic values.

Seed region	Connected region	MNI coordinates			BA	t-value	K_{extend}
		x	y	z			
VTA	PCC	4	-54	16	R 23	4.70	550
	PCC	-6	-62	22	L 31	4.23	93
LC	PFC	34	50	8	R 10	4.76	144
	PFC	22	52	-8	R 10	4.36	66
	Brainstem	-6	-18	-20	-	4.51	75
MR	Cerebellum, Right V	16	-50	-14	-	4.75	88
	Cerebellum, Right VI	30	-40	-38	-	4.28	320
	Cerebellum, Left VII, Crus I	-40	-56	-32	-	4.49	168
DR	Cerebellum, Right VII, Crus II	46	-48	-46	-	4.49	22

[Abbreviations: MNI: Montreal Neurological Institute; BA: Brodmann area; k_{extend} : cluster extension; L: left; R: right; VTA: ventral tegmental area; LC: locus coeruleus; MR: median raphe; DR: dorsal raphe; PCC: posterior cingulate cortex; PFC: prefrontal cortex]

Figure Legends

Figure 1: Seed areas used to assess functional connectivity of brainstem monoaminergic nuclei. Standard space seed masks of dorsal raphe (DR), median raphe (MR), ventral tegmental area (VTA), and left-right locus coeruleus (LC) were produced using the Harvard Ascending Arousal Network Atlas in MNI_1 mm space. The following MNI coordinates were used: DR $x=0, y=-32, z=-18$; MR $x=0, y=-32, z=-30$; VTA $x=0, y=-24, z=-20$; LC $x=6/-6, y=-36, z=-28$. Brainstem nuclei masks were overlaid onto the MNI_1 mm template using the *mrview* tool in MRtrix3 (A=anterior, R=right).

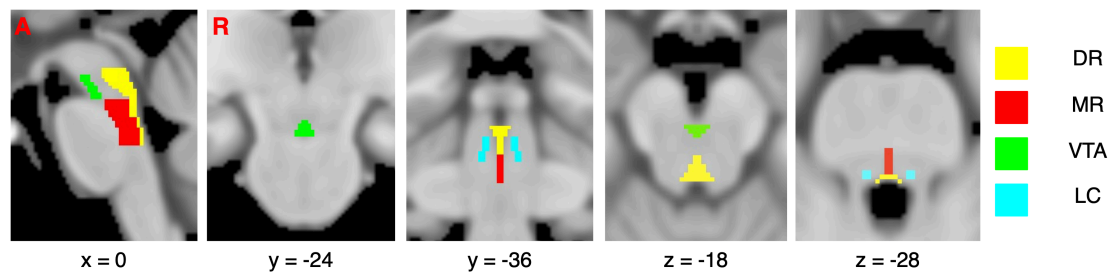


Figure 2: Patterns of brainstem monoaminergic nuclei functional connectivity in healthy controls (HC). RS-fMRI analysis showing functional connectivity between A) ventral tegmental area (VTA), B) locus coeruleus (LC), C) median raphe (MR), D) dorsal raphe (DR) and the rest of the brain in HC (main effects). Results are reported for $p < 0.001$, uncorrected, and are overlaid onto the MNI_1 mm template using the *FSLeyes* tool in FSL (R = right).

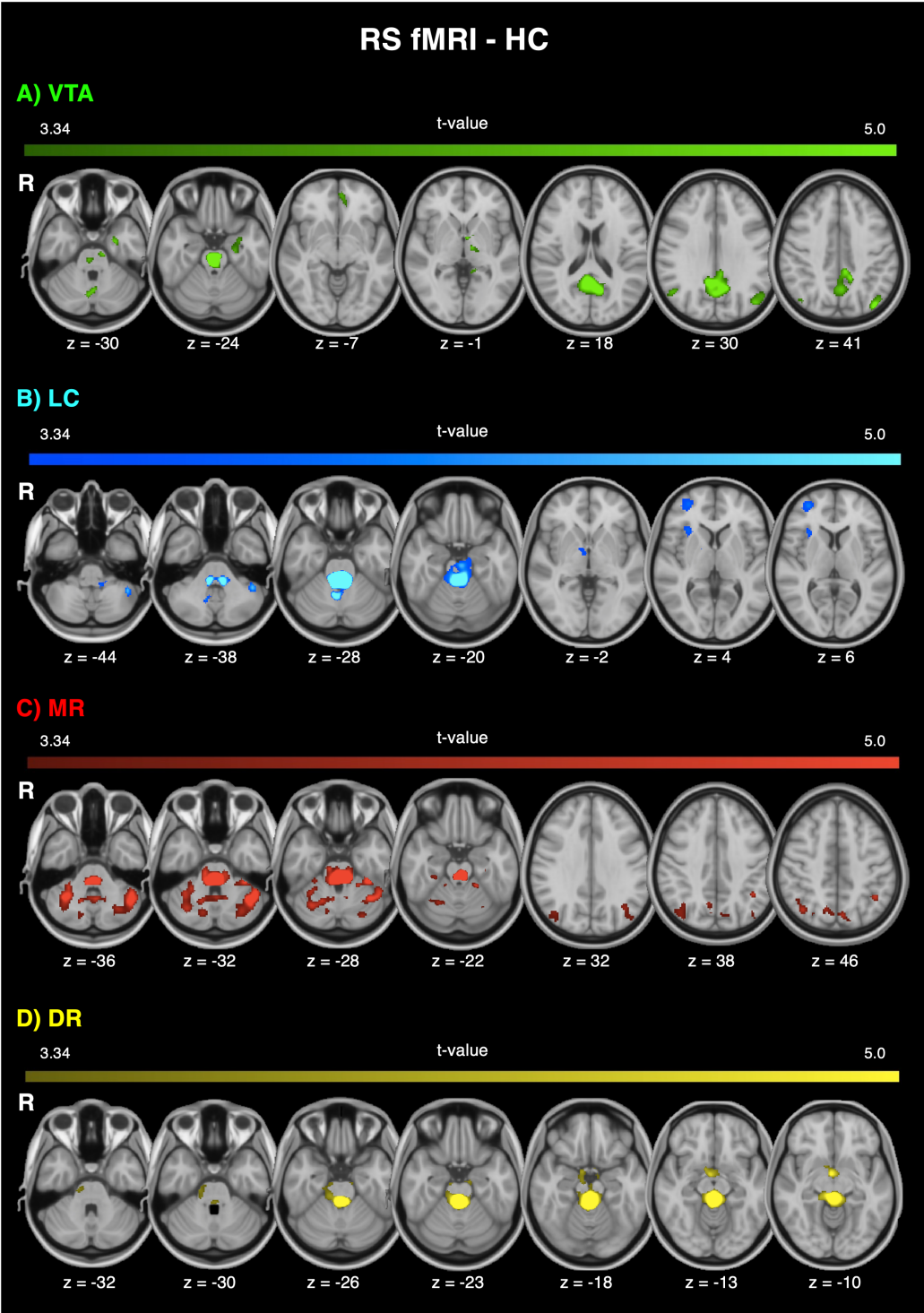


Figure 3: Dysregulation of brainstem monoaminergic nuclei functional connectivity in MS. Reductions of A) ventral tegmental area (VTA), B) locus coeruleus (LC), C) median raphe (MR), and D) dorsal raphe (DR) functional connectivity in MS-patients as compared to healthy controls (RR-MS<HC). Comparisons were carried out within the main effect of HC, setting $p < 0.05$ family-wise-error (FWE) corrected at peak level. Results are overlaid onto the MNI_1 mm template using the *FSLeaves* tool in FSL (P = posterior, R = right).

